

AD-766 698

KINETICS OF HYDRAZINE DECOMPOSITION ON
IRIDIUM AND ALUMINA SUPPORTED IRIDIUM
CATALYSTS

Owen I. Smith, et al

Air Force Rocket Propulsion Laboratory
Edwards Air Force Base, California

August 1973

DISTRIBUTED BY:



National Technical Information Service
U. S. DEPARTMENT OF COMMERCE
5285 Port Royal Road, Springfield Va. 22151

AD 766698

KINETICS OF HYDRAZINE DECOMPOSITION ON IRIDIUM AND ALUMINA SUPPORTED IRIDIUM CATALYSTS

OWEN I. SMITH AND WAYNE C. SOLOMON
AIR FORCE ROCKET PROPULSION LABORATORY
EDWARDS, CALIFORNIA 93523

Reproduced by
NATIONAL TECHNICAL
INFORMATION SERVICE
U.S. Department of Commerce
Springfield, VA 22151

AUGUST 1973

FINAL REPORT FOR PERIOD JULY 1971-JUNE 1973

APPROVED FOR PUBLIC RELEASE:

DISTRIBUTION UNLIMITED

AIR FORCE ROCKET PROPULSION LABORATORY
DIRECTOR OF SCIENCE AND TECHNOLOGY
AIR FORCE SYSTEMS COMMAND, USAF
EDWARDS, CALIFORNIA 93523

NOTICES

When U.S. Government drawings, specifications, or other data are used for any purpose other than a definitely related Government procurement operation, the Government thereby incurs no responsibility nor any obligation whatsoever, and the fact that the Government may have formulated, furnished, or in any way supplied the said drawings, specifications, or other data is not to be regarded by implication or otherwise, as in any manner licensing the holder or any other person or corporation, or conveying any rights or permission to manufacture, use or sell any patented invention that may in any way be related thereto.

UNCLASSIFIED

SECURITY CLASSIFICATION OF THIS PAGE (When Data Entered)

UNCLASSIFIED

SECURITY CLASSIFICATION OF THIS PAGE (When Data Entered)

Catalyst attrition mechanisms in monopropellant hydrazine engines are discussed in the light of this kinetic behavior. Recommendations are made concerning further elucidation of basic processes taking place in monopropellant engine cold starts.

FOREWORD

The work described in this report was accomplished under the Air Force Rocket Propulsion Laboratory's in-house Project No 573006CH, "Monopropellant Hydrazine Kinetics." This document represents the final report for the project.

The mechanism and kinetics of heterogeneous hydrazine decomposition are discussed. Results are related to proposed failure mechanisms in monopropellant engines.

The authors gratefully acknowledge the contributions of Mr. M.A. Abrego, Dr. J.A. Blauer and Dr. A.S. Kesten to various phases of this work.

This technical report has been reviewed and is approved.

PAUL J. DAILY, Colonel, USAF
Chief, Technology Division
Air Force Rocket Propulsion Laboratory

TABLE OF CONTENTS

<u>Section</u>		<u>Page</u>
I	INTRODUCTION.....	5
II	EXPERIMENTAL PROCEDURE	7
III	RESULTS AND DISCUSSION.....	15
	Iridium Wire.....	15
	Alumina Supported Iridium Catalyst.....	20
IV	CONCLUSIONS AND RECOMMENDATIONS.....	30
	REFERENCES.....	33
	AUTHORS' BIOGRAPHIES	34

LIST OF ILLUSTRATIONS

<u>Figure</u>		<u>Page</u>
1	Catalyst No. 3, 10 mil Iridium Wire	8
2	Catalyst No. 4, Monolithic Catalyst.....	10
3	Flow Reactor Schematic	11
4	Comparison of Diffusion and Chemical Controlled Kinetics on Iridium Wire.....	16
5	Reaction Order with Respect to Hydrazine - Iridium Wire.....	18
6	Activation Energy - Iridium Wire	19
7	Reaction Stoichiometry	21
8	Comparison of Diffusion and Chemical Controlled Kinetics on Monolithic Catalyst	22
9	Reaction Order with Respect to Hydrazine - Monolithic Catalyst	25
10	Activation Energy - Monolithic Catalyst	26
11	Hydrazine Decomposition Rate Temperature Dependence.....	28

LIST OF TABLES

<u>Table</u>		
1	Impurities in VP Grade Iridium	7
2	Operating Range of Flow Reactor	12
3	Noncondensable Gas Impurities.....	13

SECTION I

INTRODUCTION

In recent years, considerable effort has been directed toward the development of a hydrazine monopropellant engine which would be capable of reliable operation in a space environment for a period of years. Monopropellant engines currently in use generally use a Shell 405 catalyst bed (an alumina-support iridium catalyst) to decompose liquid hydrazine into gaseous nitrogen, hydrogen and ammonia. Failure of current long-life engines is attributed to the attrition of catalyst particles and the subsequent formation of bed voids which result in sudden, destructive increases in chamber pressure (spikes) and eventual loss of activity (washout) (Reference 1). Further, this process is greatly accelerated by starts from ambient temperatures.

Many mechanisms for the initiation and propagation of catalyst attrition have been proposed but, due to the difficulty encountered in isolation of individual mechanisms in an engine environment, there are few data available to guide further research. Proposed attrition mechanisms may be conveniently separated into two categories: those which are only casually related to the heterogeneous hydrazine decomposition rate and those for which a direct relationship exists. Examples of proposed mechanisms which fall into the first category include the mechanical crushing of catalyst particles resulting from the difference in thermal expansion coefficients between the engine and catalyst materials, gas dynamic erosion caused by high-temperature reaction products, and the removal of iridium (the active agent in Shell 405 catalyst) by chemical reaction (Reference 1). Mechanisms which fall into the second category include attrition due to thermal shock to individual catalyst particles, and large pressure gradients generated within the catalyst particle resulting from pore blockage by liquid hydrazine (References 1 and 2).

For reactions which exhibit a sudden, large increase in reaction rate with increasing temperature, the second category of attrition mechanisms assume increased importance relative to those of the first category. Kinetic behavior such as this could result from the irreversible adsorption of reactant or product species on a significant part of the catalytic surface. This phenomenon has been observed for the decomposition of hydrazine on polycrystalline tungsten and molybdenum film, where part of the surface (the 100 and 111 planes) is "poisoned" by irreversible dissociative adsorption of hydrazine for temperatures less than 1000°K (References 3 and 4). In addition, it should be noted that for a mono-propellant engine under cold start conditions, where an equilibrium condition exists between liquid and vapor phase hydrazine, reactant temperature undoubtedly influences the reaction rate by controlling the reactant concentration in the vapor phase.

The relative importance of these effects depends largely on the fraction of catalyst surface on which irreversible adsorption of hydrazine occurs, the activity of these sites relative to the "unpoisoned" sites, the global reaction order with respect to hydrazine, and the magnitude of hydrazine vapor pressure change with temperature. Nevertheless, the relationship observed between performance degradation and the number of cold starts for the Shell 405 catalyst indicates that any predominant mechanism for catalyst attrition is probably of the second category.

SECTION II

EXPERIMENTAL PROCEDURES

The heterogeneous decomposition kinetics of hydrazine were investigated in two phases. The first phase involved the use of 0.010 in. diameter iridium wire as a catalytic surface. Metallic iridium was chosen for use in initial experiments because of its non-porous surface, to and from which the rate of mass convection can be made fast enough to be negligible under suitable experimental conditions. Polycrystalline "VP grade" iridium wire was obtained from Materials Research Corp., Orangeburg, N.Y. Purity and major contaminants, as determined by resistivity and emission spectrometer measurements, are listed in Table 1. Typically, the wire was arranged in the geometry pictured in Figure 1.

In the second phase, hydrazine decomposition on an alumina-supported iridium catalyst was examined. A monolithic catalyst developed by Rocket Research Corp., Redmond, Wash., was utilized. The catalyst

TABLE 1. IMPURITIES IN VP GRADE IRIDIUM

<u>Impurity</u>	<u>Content (ppm)</u>	<u>Impurity</u>	<u>Content (ppm)</u>
C	10	Na	10
O	10	Ni	10
H	5	Pd	20
N	20	Pt	50
Ag		Rh	100
Al	10	Si	20
Cu	10	Ca	10
Fe	20		

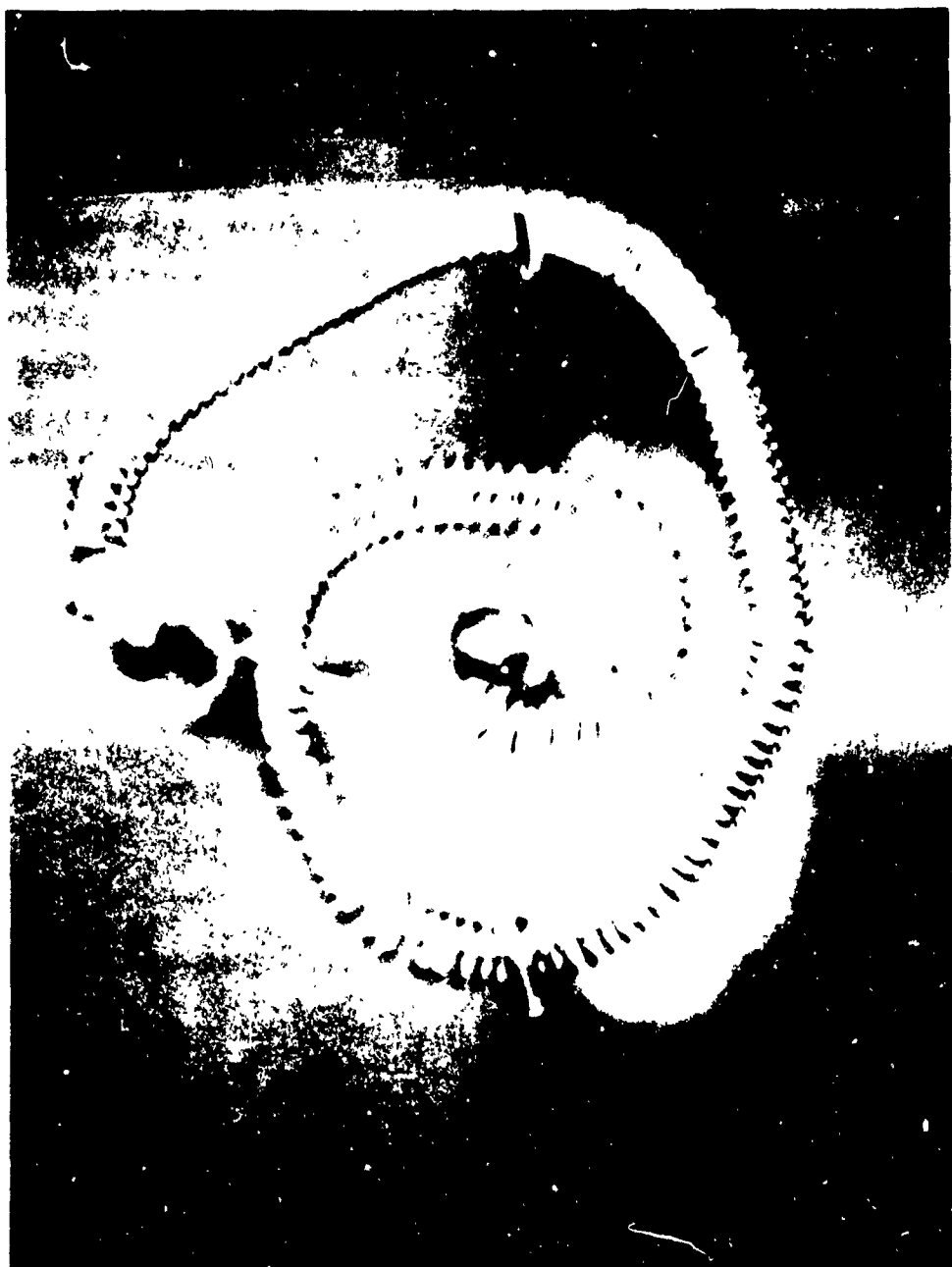


Figure 1. Catalyst No. 3, 10 mil Iridium Wire

consisted of 0.695 g of 0.020 in. diameter nichrome alloy A wire coated with 0.046 g Reynolds RA-1 aluminum oxide with a 6 wt percent silica binder. The resultant alumina surface was impregnated with 0.021 g iridium by evaporation from the chloride salt. This resulted in a surface of 31.3 wt percent iridium, and closely approximated the Shell 405 surface. Further, due to the nichrome core, resistance heating was used to control the catalyst temperature during reaction. The specific surface area of the entire catalyst (nichrome wire and surface) was determined to be $1.27 \text{ m}^2 \text{ g}^{-1}$ by interpretation of the 76°K nitrogen adsorption isotherm (BET method) (Reference 5). Catalyst samples were fabricated in a helical geometry as shown in Figure 2. Methods used in the manufacture of monolithic catalyst are further described in Reference 6.

All experiments were conducted in a flow reactor (Figure 3). In these experiments, a small amount of hydrazine (1 to 3 percent) in helium carrier gas was flowed past the catalyst sample at a pressure of 1.0 torr. After reaction, the resultant gas mixture was formed into a beam by free jet expansion through two skimmers. Since there are few collisions between molecules in the beam, atoms and unstable species live long enough to be detected by the mass spectrometer (Reference 7). The beam was directed into the ionizing region of the Bendix model 14 time-of-flight mass spectrometer nude source, operated at a typical electron energy of 17 electron volts (Reference 8).

Hydrazine concentration was monitored by means of the parent (mass 32) peak, ammonia at the parent (mass 17) peak, and nitrogen at the mass 28 peak. Hydrogen concentrations were calculated by means of mass conservation principles. The same conservation calculated was performed for nitrogen as a check against substantial error in the measurement of ammonia concentration. Operating parameters for the flow reactor are presented in Table 2.

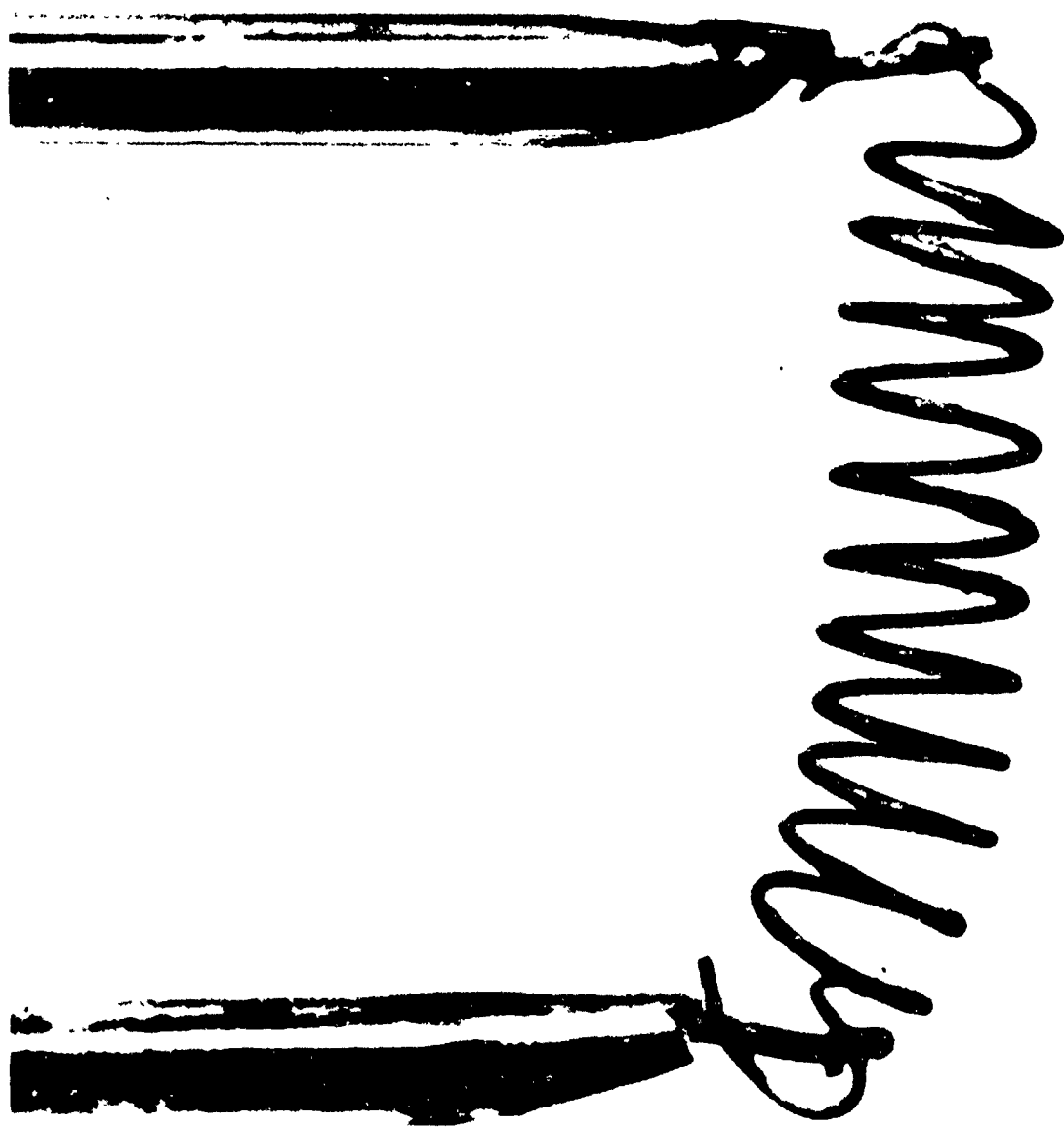


Figure 2. Catalyst No. 4, Monolithic Catalyst 0.3462 g

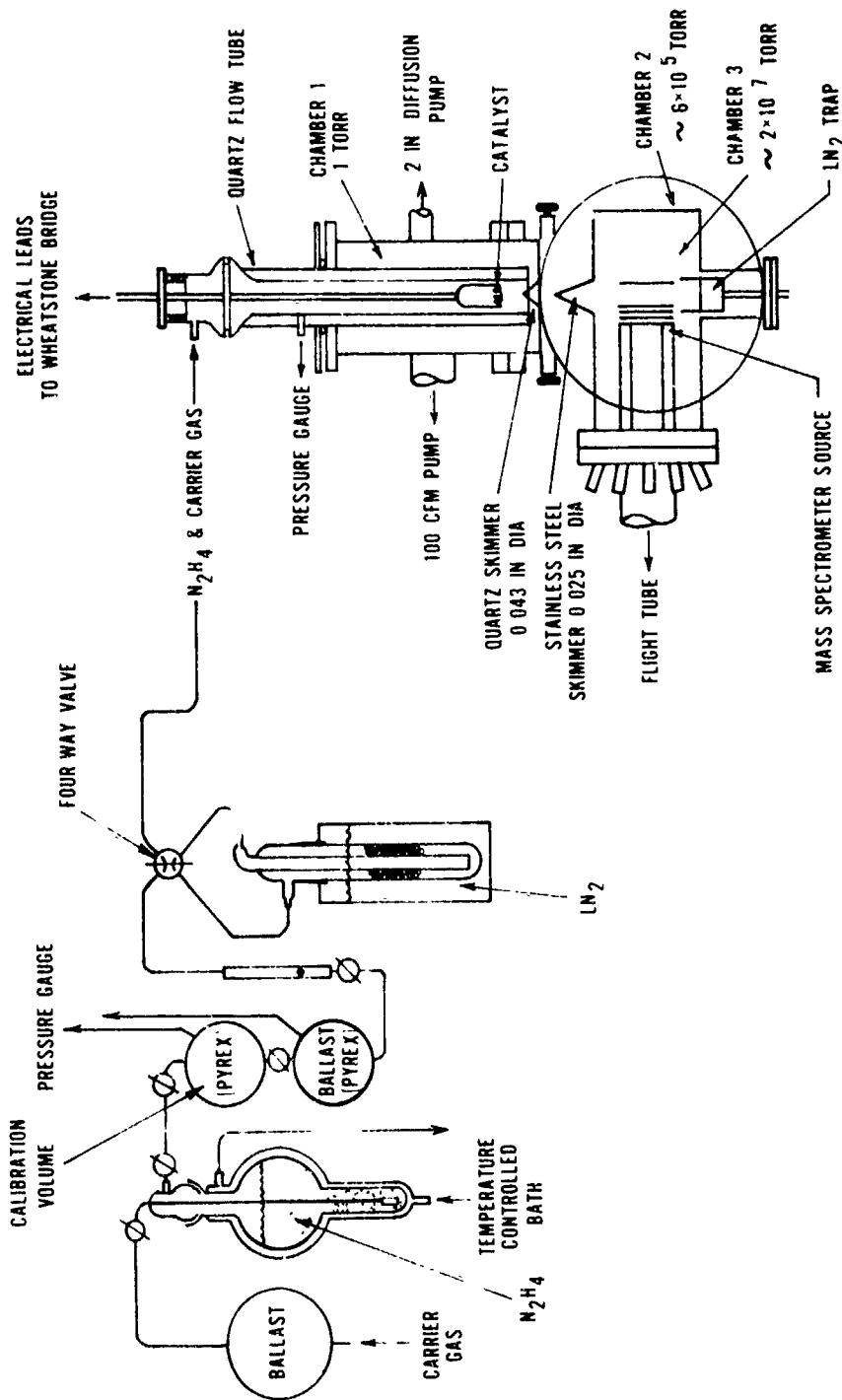


Figure 3. Flow Reactor Schematic

TABLE 2. OPERATING RANGE OF FLOW REACTOR

<u>PARAMETER</u>	<u>RANGE</u>
Carrier Gas Velocity at 1 torr	0.3 to 30 m/sec
Flow Tube Pressure	1.0 torr
Initial N_2H_4 Partial Pressure	1×10^{-2} to 3×10^{-2} torr
Carrier Gas Temperature	Ambient
Flow Tube Inside Diameter	2.68 and 3.61 cm

Catalyst temperature was maintained at the desirable level by incorporation of the catalyst sample as one arm in a Wheatstone bridge (Reference 9). The temperature resistance coefficient of each catalyst sample, along with its associated electrical leads and connections, was determined in an inert atmosphere furnace over the necessary temperature range.

Hydrazine was introduced into the flow reactor by bubbling the carrier gas through liquid hydrazine at a known pressure and temperature. Thus, the amount of reactant injected into the carrier gas stream was given by the ratio of the hydrazine partial pressure (vapor pressure) to the total pressure. Periodically, all condensable species were removed from the carrier gas by trapping at liquid nitrogen temperatures in order to determine background spectra. The quantity of hydrazine trapped during a known time interval at a known carrier gas flow rate was determined by weighing, and served as an independent measurement of initial reactant concentration.

Reaction products were introduced into the carrier gas on the downstream side of the trap from a separate flow system. A calibrated variable leak valve (Granville-Phillips) was used to regulate product flow rates. The reactant used in all experiments was propellant grade

hydrazine, further purified by distillation from barium oxide under a nitrogen blanket. The distilled hydrazine was analyzed and the major impurities were found to be 0.26 percent H_2O and approximately 0.03 percent aniline.

In addition, it should be noted that the reactant essentially undergoes another distillation during evaporation into the carrier gas, which should decrease impurity levels still further. Matheson anhydrous ammonia (99.99 percent min.) was used for the determination of reaction order with respect to ammonia. The major impurities in anhydrous ammonia are typically water and oil, both of which were largely removed by extracting the gas from the vapor phase of a relatively full bottle. Purity and major contaminant levels for all non-condensable gases used are listed in Table 3. All were used without further purification.

TABLE 3. NONCONDENSIBLE GAS IMPURITIES

<u>GAS</u>	<u>SOURCE</u>	<u>PURITY (%)</u>	<u>N (ppm)</u>	<u>O (ppm)</u>	<u>H_2O (ppm)</u>	<u>Ar (ppm)</u>
He	AFRPL Bulk	99.998	12	<4	<2	8
H_2	Matheson UHP	99.999	--	--	-	-
N_2	AFRPL Bulk	99.99	--		2	

Catalyst cleaning and pretreatment procedures were similar to those recommended by Coutour & Pannetier (Reference 10). When a new catalyst was installed in the flow reactor, it was heated to $800^{\circ}K$ in a 1 torr stream of oxygen for approximately 2 hours in order to remove any carbon-containing species from the surface. Immediately prior to the start of global rate measurements on a given day, the iridium wire catalyst was reduced at $1520^{\circ}K$ in a 1×10^{-3} torr stream of hydrogen for 15 min., flashing occasionally to more than $1770^{\circ}K$. The helium carrier gas flow was then started (the hydrazine being trapped out) at 1.0 torr and the

hydrogen flow turned off. After the residual hydrogen had been removed from the carrier gas stream, the catalyst was allowed to cool to 300°K and the experiment was begun. A similar procedure was followed using the monolithic catalyst; however, the reduction temperature was lowered to 800°K because of the fragile nature of the alumina coating. These procedures were found to yield reproducible reaction rates on each surface.

SECTION III

RESULTS AND DISCUSSION

IRIDIUM WIRE

The kinetics of hydrazine decomposition on polycrystalline iridium were determined using several lengths of 0.010 in. diameter iridium wire. Since iridium wire is essentially nonporous, theory developed for calculation of diffusion controlled reaction rates on "uniformly accessible surfaces" was applied (Reference 11). The chemical reaction at the catalyst surface was assumed to remain at equilibrium, and the reactant and product concentrations were taken from the calculated pressure equilibrium constant for the observed stoichiometry. Comparison of this calculation with experiment is illustrated in Figure 4. The ratio of the experimentally observed reaction rate to the calculated diffusion controlled rate is plotted against carrier gas velocity. Under conditions of diffusion control, this ratio should be equal to one. Results show diffusion control at velocities up to 23 m sec^{-1} for a catalyst temperature of 700°K , while the transition between diffusion and chemical control occurs at approximately 7 m sec^{-1} velocity. Similar figures were constructed to confirm chemical control for all reaction conditions. At the higher temperatures, somewhat higher flow velocities were required.

All kinetic data were subjected to a nonlinear regression analysis. The following expression for the global reaction rate was found to give good agreement with the experiment:

$$R_e = 1.74 \times 10^4 \exp \left[\frac{-(5.54 \pm 1.51) \times 10^3}{RT} \right]$$

$$[\text{N}_2\text{H}_4]^{1.39 \pm 0.31} [\text{H}_2]^{0.025 \pm 0.079} [\text{N}_2]^{-0.0001 \pm 0.098}$$

$$[\text{NH}_3]^{0.051 \pm 0.078}$$

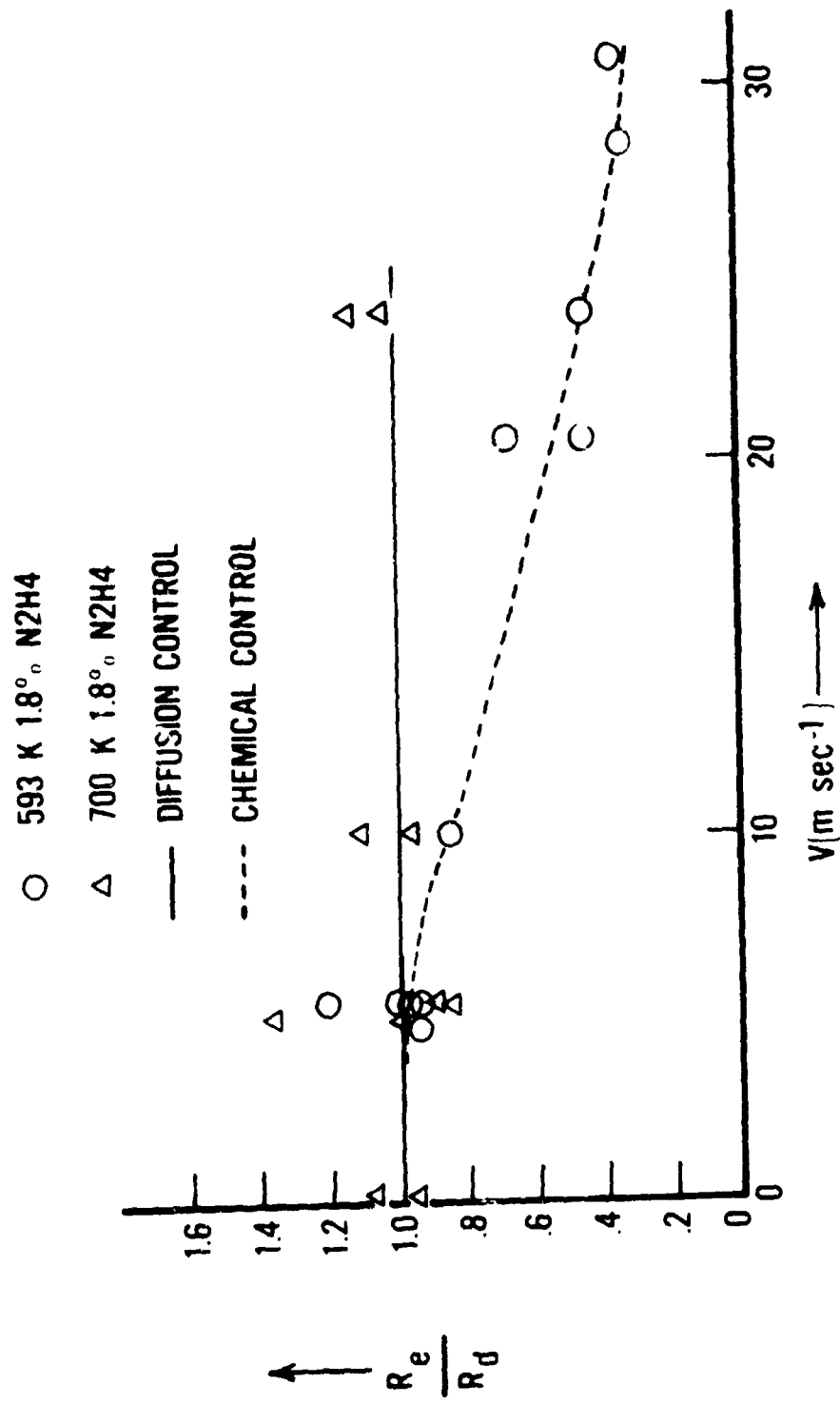


Figure 4. Comparison of Diffusion and Chemical Controlled Kinetics on Iridium Wire

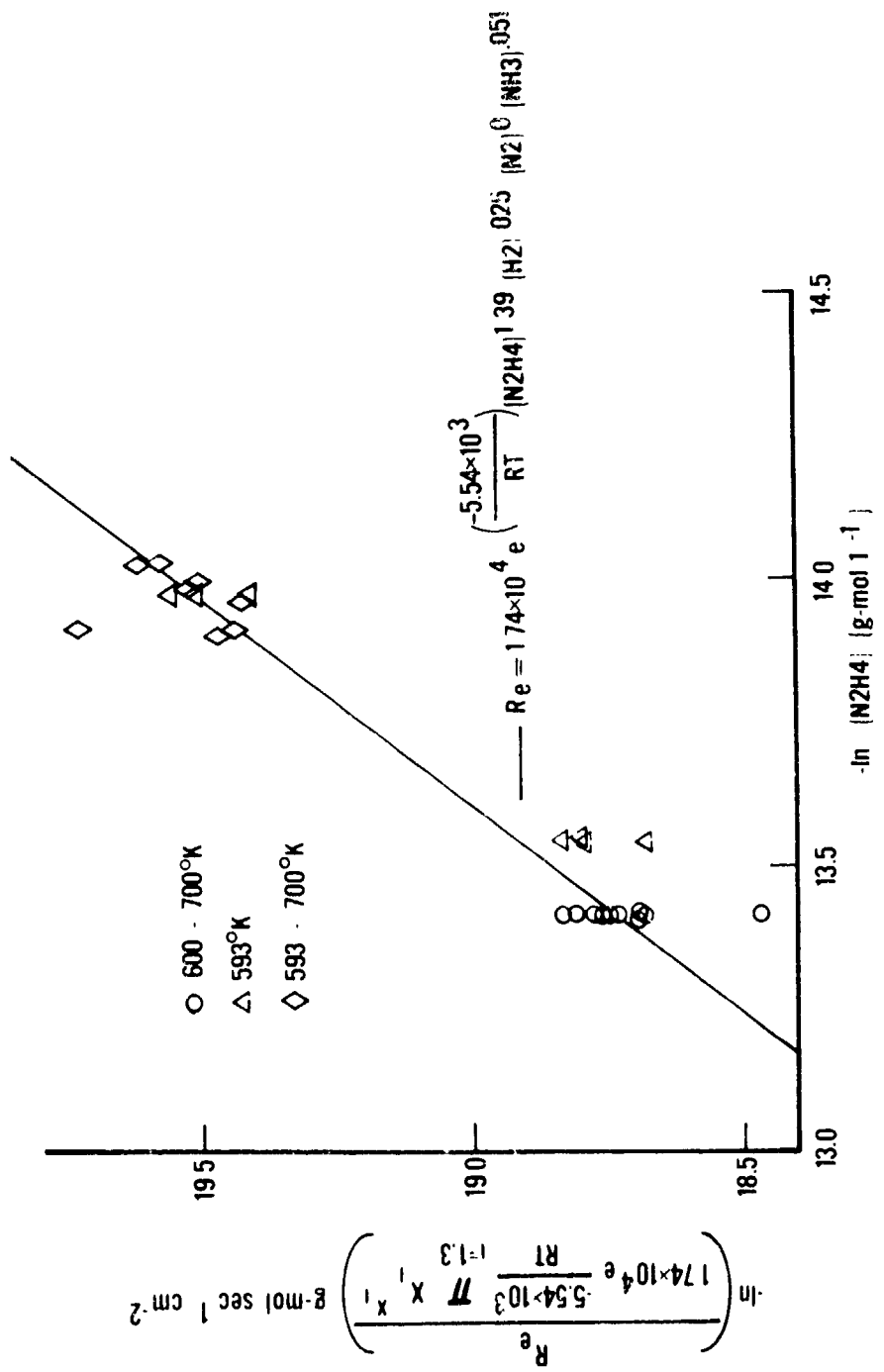
The global reaction rate for hydrazine (R_e) is in units of $\text{g-mol sec}^{-1} \text{cm}^{-2}$ (catalyst). All concentrations are in units of g-mol l^{-1} . Error limits are given for 95 percent confidence levels.

Figure 5 shows $-\ln[\text{N}_2\text{H}_4]$ plotted against a reduced function of the rate, where:

$$\prod_{i=1,3} x_i^{x_i} = [\text{H}_2]^{0.025} [\text{N}_2]^0 [\text{NH}_3]^{0.051}$$

The reaction order with respect to hydrazine was determined to be 1.39 ± 0.31 over a hydrazine concentration range of 8.11×10^{-7} to $1.96 \times 10^{-6} \text{ g-mol l}^{-1}$. Reaction orders with respect to all product species were found to be essentially zero. Product reaction orders were determined to a catalyst temperature of 593°K , over a product concentration range of 5.0×10^{-8} to $1.7 \times 10^{-6} \text{ g-mol l}^{-1}$.

The apparent activation energy for the global rate expression was found to be $5.54 \pm 1.51 \text{ kCal} \cdot \text{g-mol}^{-1}$ over a temperature range of 460 to 700°K . At a temperature of 430°K , the observed global rate was significantly lower than the value predicted from higher temperature measurements. As illustrated in Figure 6, the global rate observed at 430°K was a factor of 10 lower than the calculated rate. At temperatures of less than 415°K , the global rate was below the detection limits of the apparatus. In view of the reaction order with respect to the decomposition products, the low temperature behavior is attributed to the irreversible, dissociative adsorption of hydrazine on a significant fraction of the catalytic sites. Irreversible, dissociative adsorption of hydrazine as NH_x ($x = 0, 1, 2$) on specific crystal planes has been reported for tungsten and molybdenum (References 3 and 4).



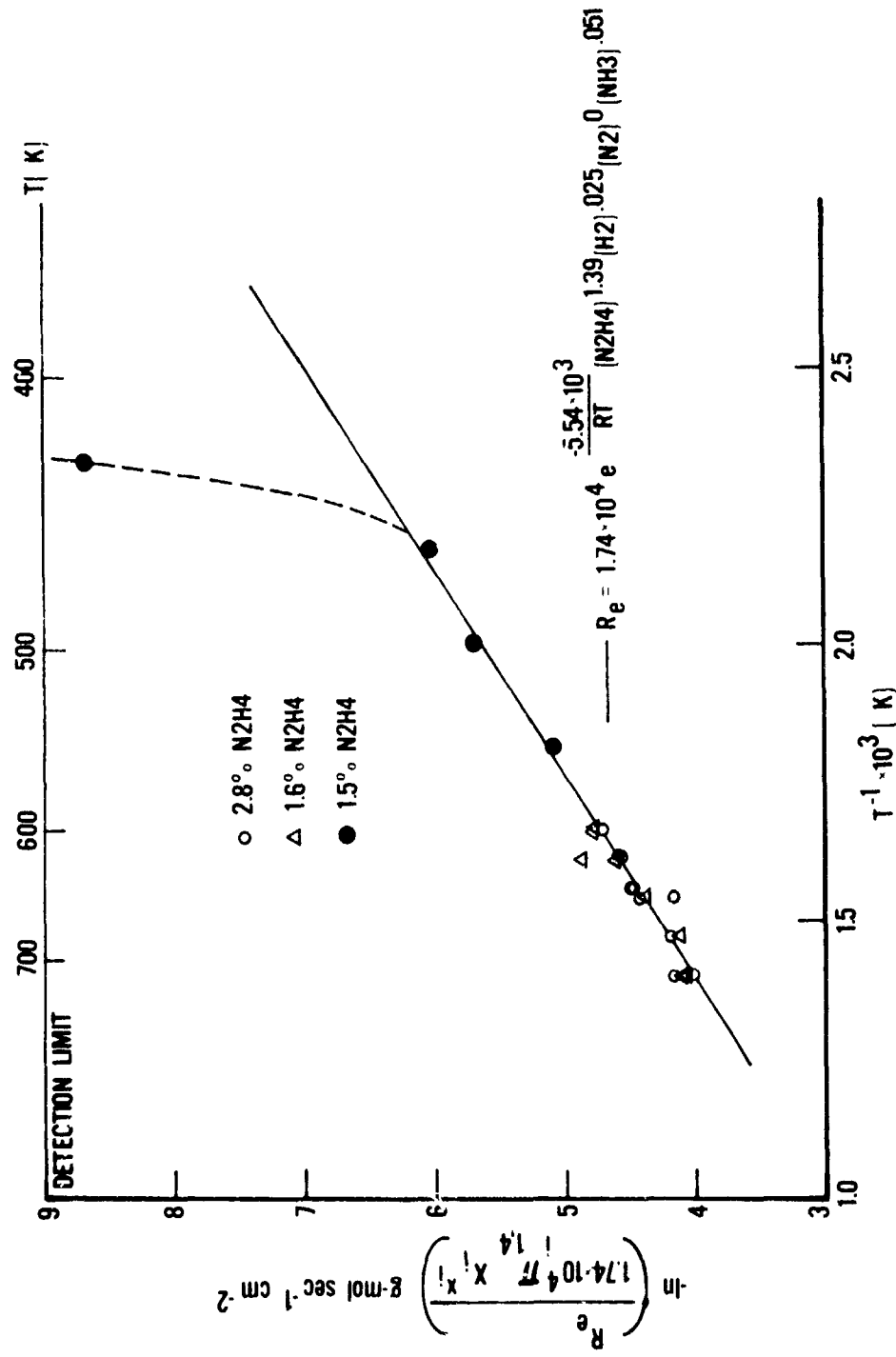


Figure 6. Activation Energy - Iridium Wire

Reaction stoichiometry was found to be dependent on catalyst temperature, as shown in Figure 7. This suggests that the decomposition of hydrazine according to the equation



first observed by Askey on heated platinum and tungsten wires may be followed by further decomposition of ammonia at temperatures in excess of 500°K (Reference 12). Since the overall reaction stoichiometry was found to be independent of carrier gas flow velocity, the secondary reaction is probably heterogeneous. This is in good agreement with Contour and Pannetier, who report the heterogeneous decomposition of ammonia on iridium powder at temperatures above 473°K (Reference 10).

ALUMINA-SUPPOTED IRIDIUM CATALYST

For a catalyst with a porous surface, the simplifying assumptions made in the calculation of diffusion rates for iridium metal are not possible.

For steady state operation, the rate of reactant diffusion to the catalyst surface is proportional to the mass-flow velocity (G) to the 0.59 power. This proportionality rises from the form of the mass transport coefficient (Reference 13):

$$K_c = 0.61 \frac{G}{\rho_i} \left(\frac{\mu_i}{\rho_i D_{AM}} \right)^{-0.667} \left(\frac{G}{A \rho \mu_i} \right)^{-0.41}$$

Under conditions of diffusion control the slope of a plot of the logarithm of the global reaction rate ($\ln R_e$) versus the logarithm of the mass flow velocity ($\ln G$) should be equal to 0.59. As shown in Figure 8, the reaction at 500°K is diffusion controlled for carrier gas velocities up to $\sim 5.4 \text{ m sec}^{-1}$ (slope = 0.57), but shows chemical control at the velocity

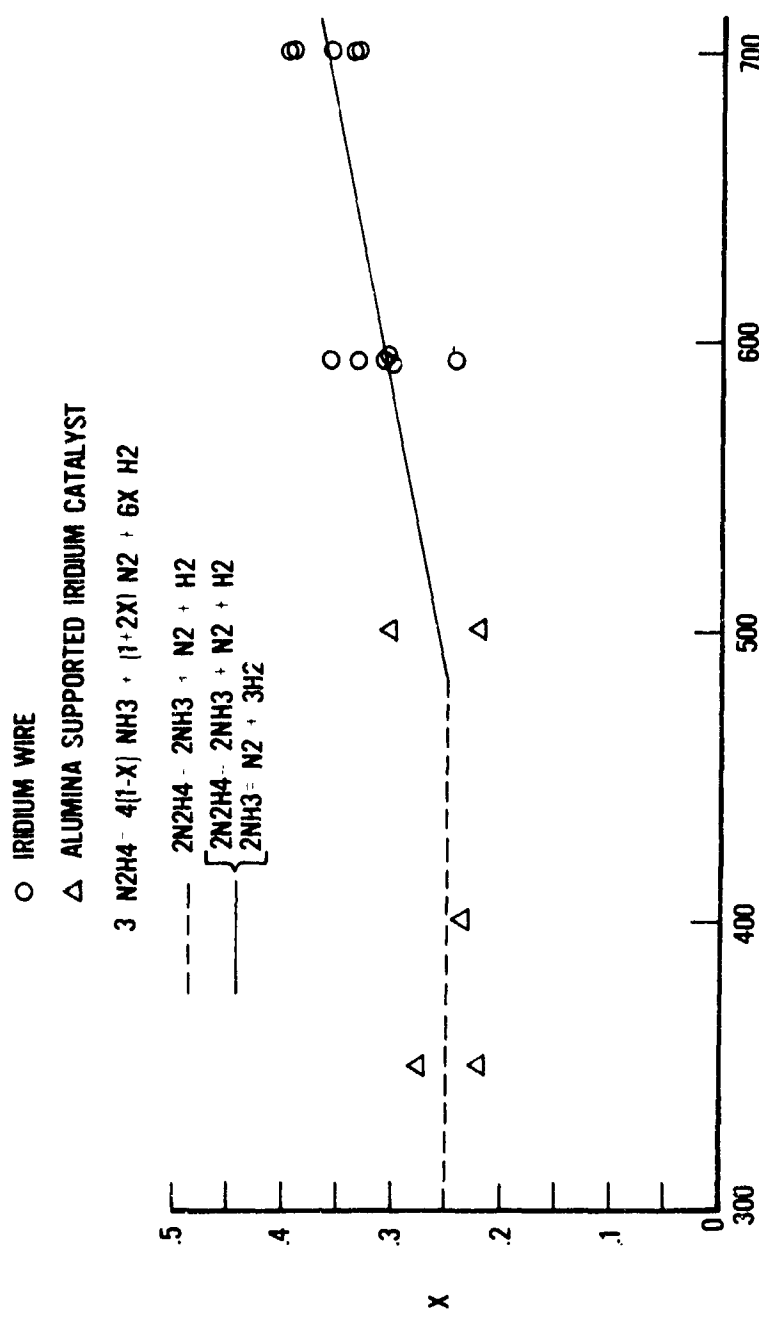


Figure 7. Reaction Stoichiometry

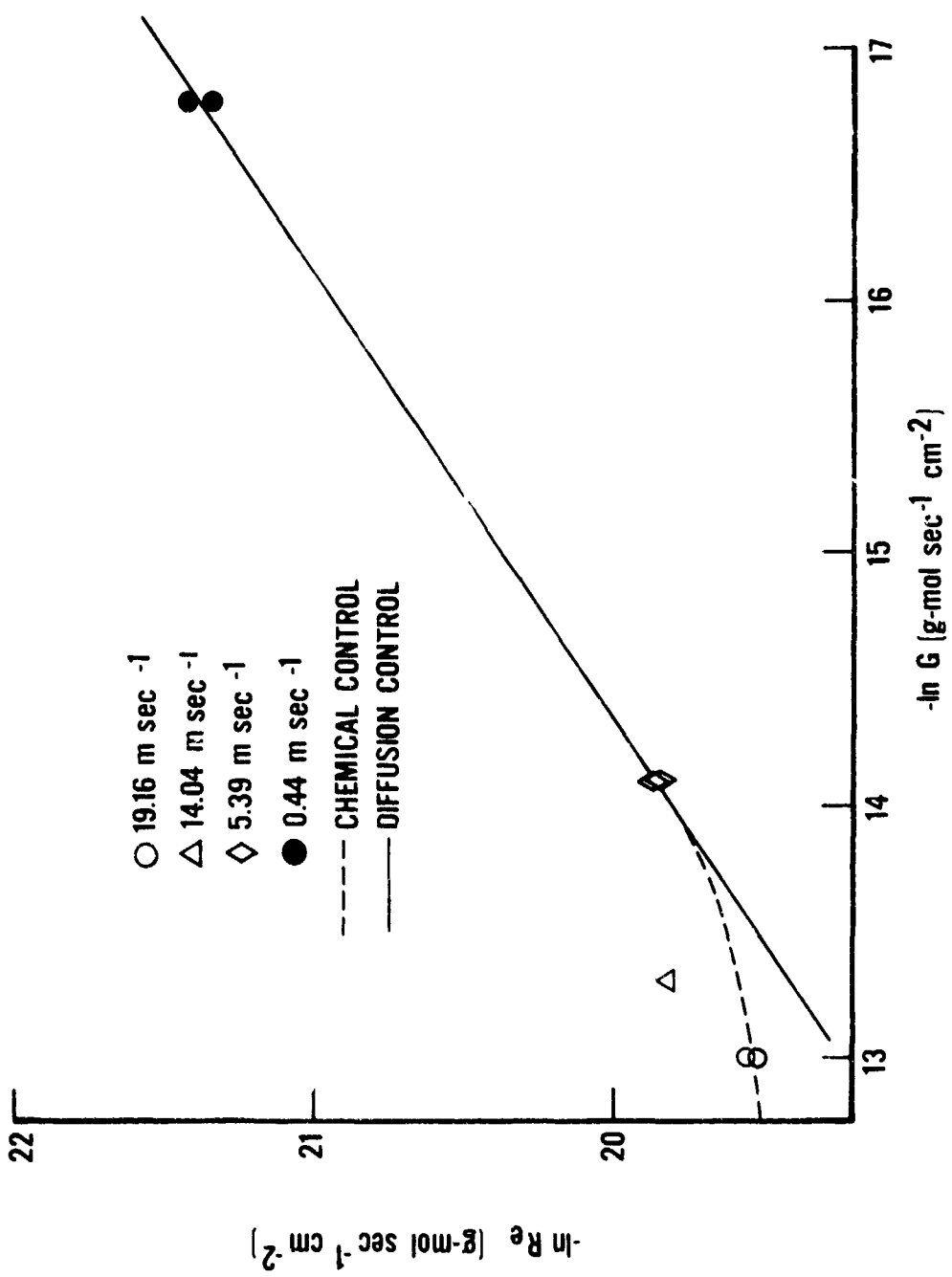


Figure 8. Comparison of Diffusion and Chemical Controlled Kinetics on Monolithic Catalyst - 500°K

of 19.2 m sec^{-1} . Accordingly, all subsequent experiments were run at velocities greater than 20 m sec^{-1} . Of course, diffusion processes taking place within the porous structure of the catalyst cannot be disregarded, but the process of mass convection from the interstitial gas to the catalyst surface is not considered under these conditions.

For the monolithic catalyst, the following expression for the global decomposition rate (obtained from nonlinear regression analysis)

$$R_e = 2.70 \times 10^{-2} \exp \left[\frac{-(1.63 \times 10^{-6} \pm 1.09) \times 10^3}{RT} \right] \\ [N_2H_4]^{1.33 \pm 0.62}$$

was found to give good agreement with the experiment. Again, the global reaction rate (R_e) is in units of $\text{g-mol sec}^{-1} \text{ cm}^{-2}$. Concentrations are in units of g-mol^{-1} and error limits are for a 95 percent confidence level.

Considerable difficulty is encountered in the comparison of the magnitude of global rates obtained on the polycrystalline iridium and monolythic catalyst surfaces. In any such comparison, the following factors must be considered quantitatively:

1. The global rate expressions were obtained over different temperature ranges. The rate expression for the polycrystalline iridium surface was determined at a temperature higher than 450°K , while the expression for the monolythic catalyst was determined below this temperature. Further, observations indicate that the rate expressions cannot be extrapolated through this temperature.
2. All global rate measurements are expressed in terms of the rate of hydrazine decomposition per unit of catalytic surface.

Comparison of such quantities pre-supposes that the entire accessible surface is covered with active metal. Electron microscope examination has shown that this is usually not the case for the alumina-supported catalyst.

3. Complex electronic interactions between the ceramic surface and iridium metal may produce sites of drastically different activity than those which exist on the bulk metal. A direct comparison between the two types of surfaces may not be valid.

Reaction order with respect to hydrazine was found to be 1.33 ± 0.62 . Agreement of experimentally obtained rates with those calculated from the global rate law is shown in Figure 9. Hydrazine reaction orders for polycrystalline iridium metal and the monolithic catalyst are essentially the same. Since the reaction on iridium metal is of zero order with respect to reaction products, an order of zero for these species was assumed for the monolithic catalyst without experimental verification.

Apparent activation energy for the reaction on monolithic catalyst was found to be near zero for catalyst temperatures between 350 and 450°K , as indicated in Figure 10. It should be noted that the slope of the line actually represents the quantity $-(E_a/\alpha R)$, where α is between 1 and 2, as opposed to the usual $-(E_a/R)$, due to the effect of the porous surface (Reference 14). As in the case of the metallic iridium surface, considerable deviation from the global rate calculated on the basis of lower temperature measurements was observed at 500°K . This behavior is attributed to the desorption of some species which is irreversibly adsorbed on a significant fraction of catalytic sites at temperatures below 450°K . Unfortunately, experimental limitations made it extremely difficult to obtain a reliable activation energy over a temperature range of less than 50°K . This fact, combined with the onset of diffusion control at a catalyst temperature slightly above 500°K , precluded determination of the apparent activation energy above 450°K .

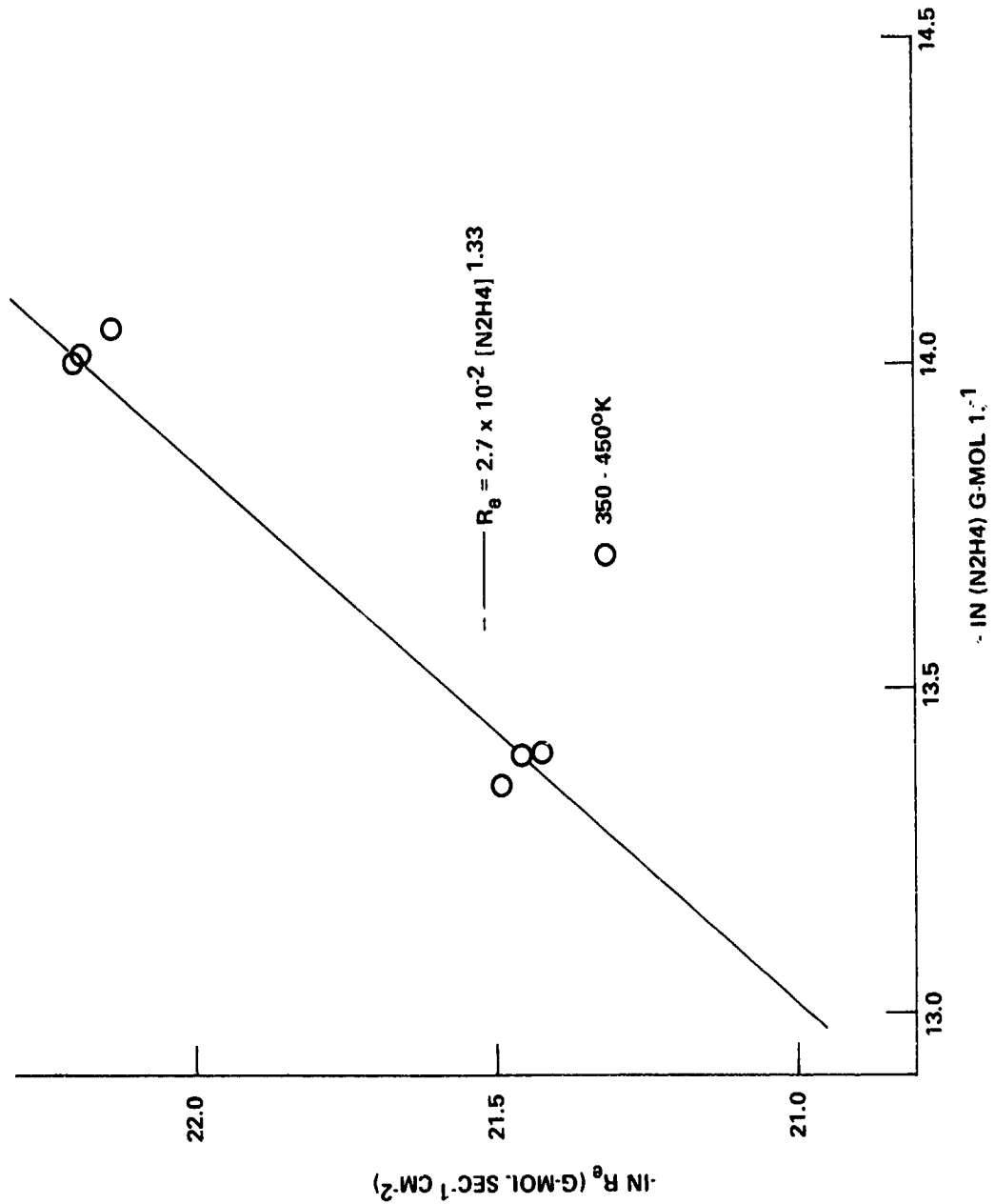


Figure 9. Reaction Order with Respect to Hydrazine - Monolithic Catalyst

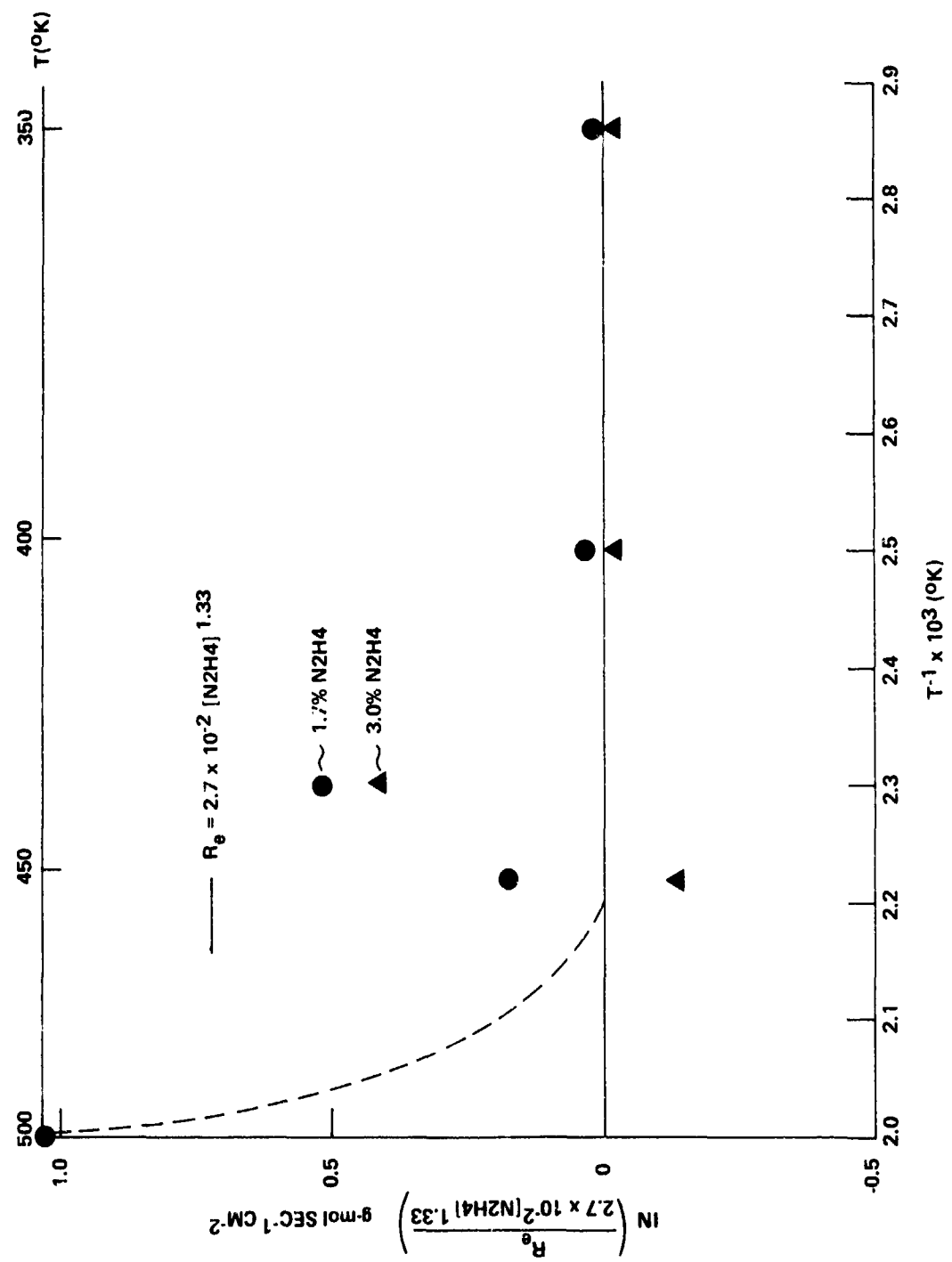


Figure 10. Activation Energy - Monolithic Catalyst

To determine the nature of the species which is apparently irreversibly adsorbed on at least part of the catalyst surface below 450°K, a qualitative flash desorption study was conducted. After cleaning the surface at 500°K, hydrazine was adsorbed at ambient temperature. Upon heating the catalyst, the desorption of ammonia along with small amounts of nitrogen was observed. At a catalyst temperature of 350°K, the desorption was slow, taking place over a period of approximately 32 sec. At 450°K, rapid desorption was observed over a period of approximately 13 sec. The zero order of the reaction with respect to ammonia on iridium metal, along with the detection of ammonia as the major desorbing species at 450°K on the monolithic catalyst indicate that the adsorbed species was probably NH₂, arising from the dissociative adsorption of hydrazine.

As indicated in Figure 7, reaction stoichiometry for hydrazine decomposition on alumina-supported iridium catalyst is identical to that for polycrystalline iridium.

The remarkably similar kinetic behavior of the decomposition reaction on polycrystalline iridium and alumina-supported iridium catalyst in the region of 450°K is illustrated in Figure 11. As noted before, only qualitative comparison of global rate magnitudes for these surfaces can be made. The dramatic change in the global reaction rate observed on each surface in the region of 450°K provides strong indication of a change in the overall nature of the catalyst passing through this temperature.

One possible explanation of this phenomenon is based on a change in the number of catalytic sites available to the reactant. According to this hypothesis, there exists on the catalytic surface at least two types of reaction sites having different kinetic behavior. One type of site is "poisoned" by the irreversible adsorption of some species at temperatures lower than approximately 450°K, resulting in its complete loss of activity,

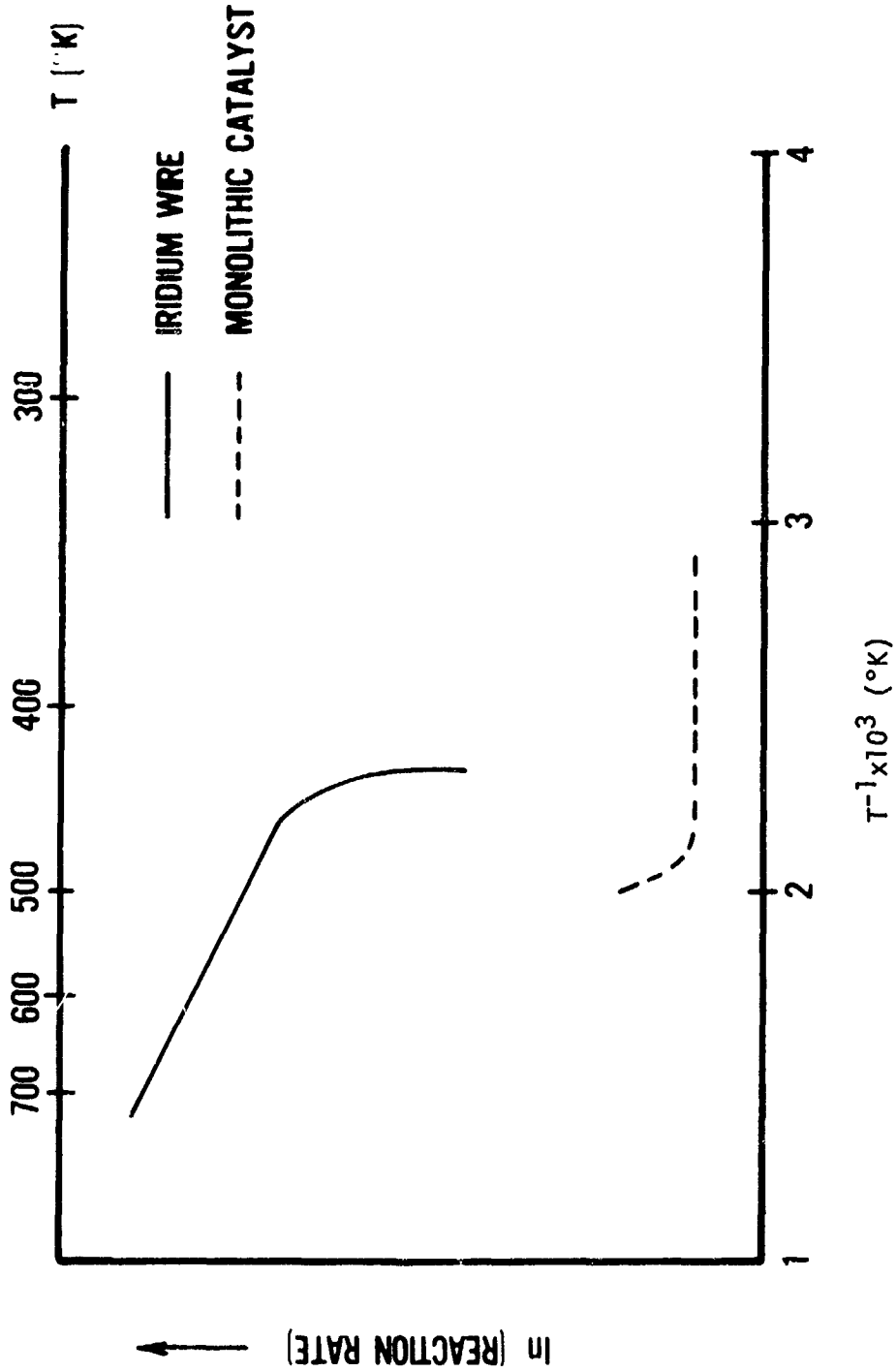


Figure 11. Pictorial Representation of Hydrazine Decomposition Rate Temperature Dependence

while the second type of site remains active in this temperature range. This dual site explanation is supported by the mechanistic study of Cosser and Tompkins on tungsten films, and by that of Contour and Pannetier on iridium powder and an alumina-supported iridium catalyst (References 3 and 10).

Alternatively, the shape of Figure 11 may be explained in terms of a change in the nature of the active sites, as opposed to their number, in the region of 450°K. In this theory, the low temperature reaction takes place on a surface covered with a monolayer or more of some species, probably NH₂. The high temperature reaction takes place in the adsorbed monolayer, and at a considerably faster rate due to the change in the electronic nature of the catalytic surface.

SECTION IV

CONCLUSIONS AND RECOMMENDATIONS

From the kinetic data gathered on the heterogeneous decomposition of hydrazine, it is clear that a process occurs on alumina-supported iridium catalyst (such as Shell 405) which could lead to drastic increases in global reaction rate at approximately 450°K. This change occurs when ammonia is desorbed from a significant part of the catalytic surface, thereby changing the number or nature of catalytic sites and resulting in an increased rate of hydrazine decomposition. Due to the fact that the absolute magnitude of this effect has not been determined, no estimate of the importance of this phenomenon relative to other rate influencing parameters in the engine (i.e., N_2H_4 vapor pressure) can be made.

The results obtained from these experiments clearly indicate the need for future work in several areas. First, more data are needed on the decomposition kinetics of hydrazine on both iridium and alumina-supported iridium catalysts. Catalyst temperatures in the range of 400 to 500°K should be emphasized. In the study just completed, the decomposition kinetics have been quantitatively determined only for temperatures in excess of 460°K in the case of the iridium catalyst, and for temperatures of less than 450°K for the monolithic catalyst. Effort should be made to extend the data through 450°K for each catalyst, as knowledge of the magnitude of the global rate change in this region is needed to evaluate its importance in catalyst attrition. This may well require two different experimental techniques, as the problem in the case of metallic iridium is to include a sufficient quantity of active sites so that the reaction can be detected at low temperatures; while in the case of the alumina-supported iridium catalyst, the problem is to eliminate diffusion control at higher temperatures.

Provided that the change in global kinetics observed at approximately 450°K is found to be significant relative to other rate influencing parameters (i.e., N₂H₄ vapor pressure) and processes (i.e., mass convection) in the engine, an effort should be made to determine the location of the species adsorbed on the surface below this temperature. If the adsorbed species covers only a part of the surface, the nature of these "poisoned" sites should be investigated. Specifically, it should be determined whether the "poisoned" sites can be attributed to different reaction mechanisms on different crystal planes of iridium or to the different electronic properties of an iridium-alumina complex and the bulk metal (References 3 and 10).

One promising method for obtaining such information is by examining the same surface by Auger-electron spectrometry and low-energy electron diffraction techniques. An apparatus which may be used to examine adsorbed species on individual crystal planes has been described recently in the literature by Ignatiev (Reference 15). Generally, Auger-electron data yield information about the adsorbed species and the nature of its bond to the surface, while the low-energy diffraction data furnish information as to the location of the adsorbed species.

If the existence of the bulk iridium agglomerates on certain crystal planes can be shown to lead to catalyst attrition, there exists a real possibility that changes in catalyst preparation can be made to largely eliminate the offending sites. In case of "poisoning" of certain iridium crystal planes, an examination of the thermodynamics and kinetics of crystal growth should result in catalyst preparation conditions that minimize the area of the offending plane. If iridium agglomeration on the substrate is found to cause catalyst attrition, several new methods for insuring a relatively even distribution of metals over ceramic surfaces may be tried.

REFERENCES

1. S.C. DeBrock, private communication, Dec. 1972.
2. A.S. Kesten, Monopropellant Specialist Session, JANNAF Propulsion Meeting, New Orleans, LA, Nov. 1972.
3. R.C. Cosser and F.C. Tompkins, Trans. Faraday Soc., 67, 526 (1971).
4. R.C.A. Contaminard and R.C. Tompkins, Trans. Faraday Soc., 67, 545 (1971).
5. S. Brunauer, P.H. Emmett, and E. Teller, J. Am. Chem. Soc. 60, 309 (1938).
6. Contract NAS7-755, NASA CR 122644, Apr. 1971.
7. W.C. Solomon, K.H. Homann, J.H. Warnatz, Int. J. Chem. Kinetics, II, 457 (1970).
8. K.H. Eberius, K. Hoyermann and H. Gg. Wagner, Thirteenth Symposium (International) on Combustion, p. 713, The Combustion Institute (1971).
9. B.J. Wood and H. Wise, J. Chem. Phys., 65, 1976 (1961).
10. J.P. Contour and G. Pannetier, J. of Catalysis, 24, 434 (1972).
11. J.M. Smith, Chemical Engineering Kinetics, McGraw Hill Book Co., Inc., New York, 1956.
12. P.J. Askey, J. Am. Chem. Soc., 52, 970 (1930).
13. R.B. Bird, W.E. Stewart, E.N. Lightfoot, Transport Phenomena, John Wiley and Sons, Inc., New York, 1960.
14. A. Clark, "The Theory of Adsorption and Catalysis," Academic Press, N.Y., 1970.
15. A. Ignatiev, American Laboratory, 5, 12 (1973).

Preceding page blank

AUTHORS' BIOGRAPHIES

OWEN I. SMITH

B.S. Chemistry, Colorado College, 1968

Project Scientist, Air Force Rocket Propulsion Laboratory, 1969-1973,
research on surface chemistry and heterogeneous combustion kinetics.

Research Fellow, University of California at Berkeley, Department of
Mechanical Engineering, 1973-present.

WAYNE C. SOLOMON

B.S. Chemistry, Idaho, 1955

PhD. Chemistry, Oregon, 1963

Development Chemist, Shell Chemical 1955-58, analysis of bio-active
organic materials and process development.

Teaching and Research Fellow, University of Oregon, 1959-63, research
on kinetics and mechanism of cycloaddition reactions.

Senior Project Scientist, Air Force Rocket Propulsion Laboratory,
1963-67, research on kinetics and combustion of fluorinated compounds.

Exchange Scientist, Institute Für physikalische Chemie, Göttingen,
1967-69, research on atom-molecule kinetics in combustion reactions
of rocket nozzles.

Chief, Kinetics, AFRPL, 1969-73, combustion kinetics of excited states
and reactions in chemical lasers.

Director, High Energy Laser Technology, Bell Aerospace Corp.,
Buffalo, N.Y., 1973-present.